Biophysical Chemistry 3 (1975) 35–45

THE SELF-ASSOCIATION OF ATP: THERMODYNAMICS AND GEOMETRY

Maarten P. HEYN and Rolf BRETZ
Department of Biophysical Chemistry, Biozentrum der Universität Basel, CH-4056 Basel, Switzerland

Received 23 April 1974
Revised manuscript received 4 September 1974

The concentration and temperature dependence of the self-association of adenosine-5′-triphosphate (ATP) in aqueous solution was studied by means of ultraviolet absorption spectroscopy and circular dichroism (CD). Of several possible models, a model with indefinite linear self-association, in which each step has the same equilibrium constant, describes the data best. The two different methods lead within experimental error to the same thermodynamic parameters. At pH 8.7, in 1 M Tris and 0.5 M $MgCl_2$, we find $\Delta H^0 = -5.1$ kcal/mole and $\Delta S^0 = -13.0$ e.u. These values do not differ much from those found for the self-association of uncharged bases and nucleosides in aqueous solution. The CD spectrum that results from the self-association is conservative and quite similar in shape to that observed for some stacked dinucleotides; it is interpreted as a first approximation within the framework of the exciton model.

1. Introduction

The self-association of nucleic acid bases, nucleosides and nucleotides has been studied by various methods. The field was recently reviewed by Ts'o [1]. In aqueous solution the aggregation is thought to occur via vertical stacking between the bases. There appears to be very little previous work on the self-association of the charged nucleotides in aqueous solution. For adenosine-5′-monophosphate (AMP), the NMR work by Ts'o [2] and the ultracentrifuge study by Rossetti and Van Holde [3] show that these particles associate beyond the dimer stage. The thermodynamic parameters could not be determined, however. We have studied the self-association of ATP as a function of temperature and concentration by ultraviolet difference absorption spectroscopy (UV) and CD difference measurements, with the goal of obtaining the thermodynamic parameters and gaining structural information on the mode of stacking.

The absorption difference between two cells, each containing the same number of ATP molecules in the beam area – one short and filled with a concentrated partially aggregated ATP solution, the other long and filled with a diluted not-aggregated ATP solution – was directly determined. For the CD measurements this difference was determined by numerically subtracting the corresponding spectra. These difference signals can be expressed as a function of the total weighed-in ATP concentration and are a convenient measure for the extent of association. By measuring these difference signals as a function of the two parameters, temperature and concentration, over the ranges −2°C to 48°C and 0.01 M–0.1 M, the thermodynamic parameters for the stacking process could be determined.

Some of these results are independent of any model assumptions, others depend on the particular thermodynamic model chosen to describe the self-association and on the dependence of the optical parameters on the length of the aggregate. The least squares criterion was used to distinguish between various models. If ATP self-associates by vertical stacking, one may expect to see typical couplet type CD difference spectra; this was indeed observed. The temperature dependence of the rotational strength was used to determine the thermodynamic parameters, which agreed with those determined by absorption spectroscopy. The amplitude of the CD signal contains information on the stacking geometry and was interpreted in terms of the angle between the transition dipole moments of the 259 nm transition in neighboring monomers.

2. Self-association models

In the first part of this section we will discuss thermodynamic models for self-association. In the second and third part we will consider the way in which the optical signals depend on the extent of self-association, and the dependence of the CD signal on the self-association geometry.

The literature on self-association models was recently reviewed by Magar [4]. Much of the original work is due to Kreuzer [5], Schellman [6], Ts'o and Chan [7], and Steiner [8]. We will briefly review some aspects of these theories. This also serves the purpose of defining the quantities needed later on. The self-association of a molecule A into aggregates of various sizes is described in a rather general way by the following set of equilibria:

$$A_1 + A_1 \overset{K_2}{\rightleftarrows} A_2,$$

$$A_2 + A_1 \overset{K_3}{\rightleftarrows} A_3,$$

$$\vdots$$

$$A_{i-1} + A_1 \overset{K_i}{\rightleftarrows} A_i,$$

$$\vdots$$

In this reaction scheme A_1 represents the monomer, A_i stands for an aggregate consisting of i monomers. Such a model contains too many parameters to be determined experimentally if extensive aggregation occurs. On the other hand one should ask whether it is physically reasonable to have a different equilibrium constant for each step. Molecules with large planar ring structures, such as ATP, most likely aggregate by base stacking, i.e., linear aggregates are formed. For uncharged bases and nucleosides very short range forces are involved here and it is thus unlikely that K_i will depend strongly on i. For charged nucleotides in solutions of high salt concentration, such as the system under study, there are in addition screened Coulomb interactions which may lead to some i-dependence of K_i. At pH 8.7, ATP is fourfold negatively charged, and estimates of the screening length for this species at the salt concentration used show that the charge repulsion effect upon aggregation is small. A next nearest neighbor interaction cannot be completely excluded, however. We will therefore consider two models with indefinite self-association. In the first model all equilibrium constants are equal: $K_1 = K_2 = K_3 = \ldots = K$. In the second model only K_1 differs from all the other equilibrium constants: $K_2 = K_3 = \ldots = K$ and $K_1 = \sigma K$. The first model is of course the case $\sigma = 1$ of the more general second model. When $\sigma < 1$ we would call the system cooperative since the aggregation is enhanced once a dimer is formed. The case $\sigma > 1$ would be called anticooperative. One may expect that $\sigma \geqslant 1$ for the system under study. We also considered the dimer case in detail. Physically there is no good reason why the association would abruptly end at $i = 2$. On the other hand such a model may be useful to describe the data at low concentration.

Let c be the total weighed-in concentration of ATP and c_i the molar concentration of the aggregate consisting of i monomers. Mass conservation can be written as

$$c = \sum_{i=1}^{\infty} i c_i \tag{1}$$

for the case of indefinite self-association, and as

$$c = c_1 + 2c_2$$

for the case of dimerization. For the model with $\sigma \neq 1$, we have according to the law of mass action:

$$c_2 = \sigma K c_1^2; \quad c_i = \sigma K^{i-1} c_1^i, \quad i \geqslant 2.$$

Introducing the convenient dimensionless variables

$$L = Kc,$$

and

$$s = Kc_1,$$

the summation in eq. (1) can be carried out leading to

$$L = s - \sigma s + \sigma s/(1-s)^2. \tag{2}$$

By setting σ equal to one we arrive at the corresponding relationship for the non-cooperative model:

$$L = s/(1-s)^2. \tag{3}$$

For the dimer case we get

$$L = s(1+2s). \tag{4}$$

So far the effects of non-ideality have been neglected. In a more general treatment the law of mass action should be formulated with activities instead of concentrations. The activity of the aggregate with i monomers, a_i, can be written as a product of c_i and an activity coefficient γ_i:

$$a_i = c_i\gamma_i.$$

Adams and Williams [9] proposed the following expansion for γ_i:

$$\ln \gamma_i = B_1 M_i c + B_2 M_i c^2 + \dots, \tag{5}$$

in which M_i is the molecular weight of A_i. This expansion has frequently been used in studies on self-association. When the non-ideality can indeed be described by (5), one can easily show that

$$\gamma_i = \gamma_1^i,$$

and eqs. (2), (3) and (4) remain correct.

We now have to consider the contribution of aggregates of various lengths to the optical signals. When a dimer is formed in which the chromophores of the monomers stack, the absorption spectrum changes due to the interaction between the excited states in the presence of the electromagnetic field. A third monomer aggregating with this dimer to form a trimer causes an additional change. When two planar chromophores stack in such a way that the resulting aggregate is "asymmetric", a rotatory strength couplet is induced which is due to the interaction between the transition dipoles in the two chromophores [10, 11].

A simple phenomenological description for the i-dependence of the extinction coefficient of the aggregates, consistent with the assumption that only nearest neighbor interactions are responsible for the change in optical parameters, is the following

$$\epsilon_i = 2\epsilon_e + (i-2)\epsilon_{int}, \quad i \geq 2, \qquad \epsilon_1 = \epsilon_m. \tag{6}$$

In this expression ϵ_m is the free monomer extinction coefficient, ϵ_e is the extinction coefficient of a monomeric unit at the end of an aggregate and ϵ_{int} is the extinction coefficient of an internal unit. Similar expressions have been proposed before for aggregating systems [12, 13]. Oligonucleotides, which can to some extent be considered as covalent analogs of the aggregates, have optical properties consistent with this expression [14]. For the optical density of a cell of thickness d (cm), filled with partially self-associated molecules at total monomer concentration c, we may now write

$$E = d\sum_{i=1}^{\infty} c_i\epsilon_i = d\left(\epsilon_m c_1 + 2\epsilon_e \sum_{i=2}^{\infty} c_i + \epsilon_{int}\sum_{i=2}^{\infty}(i-2)c_i\right) \tag{7}$$

In the reference cell, we would like to have all molecules in the unassociated state. This can be simply achieved by taking a reference cell of length d_m, much longer than d, filled with a diluted solution of concentration c_m, with

$$dc = d_m c_m$$

such that at concentration c_m all molecules are in the monomer state.

In a Gedanken-experiment we may think of taking the cell filled with self-associated particles, and transforming it into the reference cell by increasing its length and filling it up with solvent until the solution is so far diluted that no self-association is present any more. In both cells the beam will be presented with the same number of monomers per cm^2 of area perpendicular to the beam direction. The optical density of the reference cell is thus

$$E_{ref} = d_m c_m \epsilon_m = dc\epsilon_m.$$

For the difference signal we have therefore

$$\Delta E = d\left(2(\epsilon_e - \epsilon_m)\sum_{i=2}^{\infty} c_i + (\epsilon_{int} - \epsilon_m)\sum_{i=2}^{\infty}(i-2)c_i\right). \tag{8}$$

Defining

$$\Delta\epsilon_e = \epsilon_e - \epsilon_m, \qquad \Delta\epsilon_{int} = \epsilon_{int} - \epsilon_m,$$

$$\alpha = \Delta\epsilon_{int}/\Delta\epsilon_e, \qquad \Delta\epsilon = (\Delta E)/dc,$$

we can rewrite (8) in the following way:

$$\Delta\epsilon = \Delta\epsilon_e\left(\frac{2}{c}\sum_{i=2}^{\infty} c_i + \frac{\alpha}{c}\sum_{i=2}^{\infty}(i-2)c_i\right). \quad (9)$$

For each of the three models discussed above, the sums in (9) can be evaluated. For the case of indefinite non-cooperative self-association this yields:

$$\Delta\epsilon(L) = \Delta\epsilon_e\left\{-\frac{3}{L} - \frac{1}{L^2} + \left(\frac{1}{L}+\frac{1}{L^2}\right)\sqrt{4L+1} + \alpha\left[1+\frac{2}{L}+\frac{1}{2L^2} - \left(\frac{1}{L}+\frac{1}{L^2}\right)\sqrt{4L+1}\right]\right\}. \quad (10)$$

For the case of cooperative self-association one finds:

$$\Delta\epsilon(L) = \Delta\epsilon_e\left\{\frac{2\sigma}{L}\frac{s^2}{1-s} + \frac{\alpha}{L}\left(L - s - 2\sigma\frac{s^2}{1-s}\right)\right\}, \quad (11)$$

from which s may be eliminated with the help of the cubic mass conservation equation (2). For the dimerization case one has

$$\Delta\epsilon(L) = \Delta\epsilon_e\left(1+\frac{1}{4L} - \frac{1}{4L}\sqrt{8L+1}\right). \quad (12)$$

We see that $\Delta\epsilon$ is a function of the dimensionless variable $L = Kc$, with parameters $\Delta\epsilon_e$, α and σ. Experimentally we can vary L by changing the temperature or the weighed-in concentration c. The dimer case has of course the smallest number of parameters, followed by the case of non-cooperative self-association, followed by the cooperative case. On first sight these expressions appear to be singular at $L = 0$. From the definition of $\Delta\epsilon$ as the extinction coefficient difference between an aggregated solution and a non-aggregated solution it follows that $\Delta\epsilon(0) = 0$. Since $\Delta\epsilon$ must be a continuous function of L, we have for small enough L, for any model

$$\Delta\epsilon = \epsilon_1 L + \epsilon_2 L^2 + \epsilon_3 L^3 + \ldots = A_1 c + A_2 c^2 + A_3 c^3 + \ldots, \quad (13)$$

in which $\epsilon_1, \epsilon_2, \epsilon_3$ have the dimensions of an extinction coefficient. Carrying out the Taylor series expansions of (10), (11) and (12), we find of course that no singularities occur. The expressions for A_1, A_2, and A_3 for the various models are summarized in table 1. It is clear from this table that a determination of A_1 is not sufficient to distinguish between the various models. Apart from the factor of two, A_1 is the product of $\Delta\epsilon_e$ and the dimerization equilibrium constant (K or σK). Since the first term in (13) is due to dimerization only, it is the same in all models. Subsequent terms in (13) cannot be given such a simple interpretation; to the second term in (13) for instance, one has contributions from both trimers and dimers. According to eq. (13), A_1 and A_2 can be determined by plotting $\Delta\epsilon/c$ versus c for small c (such that the expansion converges). A_1 and A_2 are the intercept and slope of the resulting straight line. Having determined A_1 in this way for a number of temperatures, one may determine ΔH^0 from the slope of the plot of $\ln A_1$ versus $1/T$:

$$\ln A_1 = \ln 2\Delta\epsilon_e + \frac{\Delta S^0}{R} - \frac{\Delta H^0}{R}\frac{1}{T}. \quad (14)$$

From the intercept one gains information on $\Delta\epsilon_e$ and ΔS^0. We wish to emphasize that the ΔH^0 so obtained is the dimerization enthalpy, and is independent of any model assumptions, since eq. (13) holds no matter which model is used. Table 1 shows that the slope A_2 should be negative for all reasonable values of α and σ.

For the CD signals similar considerations hold, and replacing everywhere ϵ by $\delta\epsilon = \epsilon_L - \epsilon_R$ eqs. (10) to (12) as well as table 1 can be used without further change.

The degenerate exciton model has been used to give a first order description of the CD spectra of those stacked dinucleotides which show conservative CD spectra [15]. Non-conservative CD spectra cannot be explained by exciton terms alone. The CD spectrum of the stacked dimer of ATP, however, is conservative for all temperatures (see fig. 5) and the sim-

Table 1
Expansion coefficients for various self-association models

Model	Dimerization	Non-cooperative indefinite self-association	Cooperative indefinite self-association
A_1	$2\Delta\epsilon_e K$	$2\Delta\epsilon_e K$	$2\Delta\epsilon_e \sigma K$
A_2	$-8\Delta\epsilon_e K^2$	$-(6-\alpha)\Delta\epsilon_e K^2$	$-(8\sigma-2-\alpha) \times \Delta\epsilon_e \sigma K^2$
A_3	$40\Delta\epsilon_e K^3$	$(18-4\alpha)\Delta\epsilon_e K^3$	–

plest theory that predicts such a spectrum is the degenerate exciton model. The interaction between excited states, induced by the aggregation of two monomers 1 and 2, leads to a splitting of the absorption band into two peaks localized at λ_+ and λ_-, with

$$\lambda_\pm = \lambda_0 \mp \frac{\lambda_0^2}{c}\frac{V_{12}}{h}.$$

In this expression λ_0 is the wavelength of the monomer absorption maximum, c the speed of light, and h Planck's constant. V_{12} is the matrix element of the Coulomb interaction between the state with the excitation on monomer 1 and the state with the excitation on monomer 2. In principle V_{12} can be calculated if one knows the ground and excited state wave functions. Often a multipole expansion for V_{12} is employed, which is usually terminated after the first term:

$$V_{12} = \frac{1}{|R_{12}|^3}\left\{\mu_1 \cdot \mu_2 - 3\frac{(\mu_1 \cdot R_{12})(\mu_2 \cdot R_{12})}{|R_{12}|^2}\right\}. \quad (15)$$

R_{12} is the distance vector from monomer 1 to monomer 2. μ_1 is the transition dipole moment vector of the 259 nm transition in monomer 1; μ_2 the corresponding quantity for the same transition in monomer 2. In cases where this termination is justified, the advantage of (15) over the calculation using wave functions is that one can employ experimentally known transition dipole moments. The rotational strength induced by the aggregation is given by

$$R_\pm = \mp(\pi/2\lambda_0)R_{12} \cdot (\mu_1 \times \mu_2), \quad (16)$$

with R_+ belonging to the band at λ_+, R_- belonging to the band at λ_-. We are assuming all bands to be gaussian. The complete CD spectrum is then given by

$$\delta\epsilon(\lambda) = \delta\epsilon_0\left\{\exp -\left(\frac{\lambda-\lambda_+}{\Delta}\right)^2 - \exp -\left(\frac{\lambda-\lambda_-}{\Delta}\right)^2\right\}. \quad (17)$$

In this expression Δ is the bandwidth of the monomer absorption spectrum. For a gaussian band $\delta\epsilon_0$ is related to R_+ by

$$R_+ = (1/2.28)(\Delta/\lambda_0)\delta\epsilon_0. \quad (18)$$

When $|\lambda_+ - \lambda_-| \ll \Delta$, expression (17) can be simplified considerably by Taylor series expansion. The shape of the CD band becomes essentially the derivative of the absorption spectrum and the position of the peaks is determined by Δ rather than by λ_+ and λ_-. In general, for the CD spectrum induced by self-association to the dimer stage, one expects a conservative spectrum, as in (17). Such a spectrum is also often called a "couplet" [10]. The amplitude of the signal contains information on the dimer geometry through eq. (16).

3. Materials and methods

The disodium salt of adenosine-5'-triphosphate was purchased from Boehringer (Mannheim, Germany). Elemental analysis showed (theoretical values in parentheses) 19.32% (19.84%) C and 3.64% (3.33%) H. The inorganic phosphate, AMP, and ADP contents were determined to be (weight percentage) 0.21%, 0.17% and 1.2%. The substance was used without further purification. Concentrations were determined spectroscopically, using a monomer extinction coefficient of 15400 M^{-1} cm^{-1} at 259 nm. Dilutions were performed with a Metrohm E 457 microburette (Herisau, Switzerland). Most measurements were performed in Tris buffer at pH 8.7 (25°C), where ATP exists exclusively in its fourfold negatively charged state.

The absorption measurements were performed on a Cary-15 spectrophotometer, equipped with thermostatable cuvette holder, which was connected to a Lauda TUK 30 thermostat. The extinction difference between probe cell and reference cell, both filled with buffer, was used as a base line. Temperatures were recorded using a calibrated thermistor. For each solution, 10 to 12 measurements were performed at 288 nm in the temperature range −2°C to 48°C. After reaching the highest temperature, reversibility was proved by cooling down to 25°C and comparing the absorbance with the value measured at this temperature in the beginning.

The CD measurements were performed on a Cary 61 over the wavelength interval 230–320 nm. The CD spectra were digitalized using a curve analyzer (Bradley Instruments) and subsequently approximated by a Fourier series by means of a Hewlett–Packard 9819 A computer. The resulting function was plotted and directly compared with the original spectrum. No

significant differences could be detected. All necessary manipulations like subtraction of base lines, scaling in concentrations and subtraction of monomer spectra were done on the vectors of Fourier coefficients. In the end the resulting spectra were resynthetized on a plotter.

4. Results and discussion

In fig. 1 the results of the absorption difference measurements at 288 nm are collected for various concentrations of ATP at pH 8.7 in 1 M Tris buffer and 0.5 M $MgCl_2$. From top to bottom the weighed-in concentration decreases from 0.1 M to 0.01 M. The data are plotted logarithmically: ln $\Delta\epsilon$ versus $1/T$. The temperature varies from left to right from 48°C to −2°C. The points can be fitted within experimental accuracy by straight least squares lines. If only the first term in (13) were to contribute (very low L), one would expect perfect Van 't Hoff behavior, with the same slope $(-\Delta H^0/R)$ for each concentration. Fig. 1 shows that from top to bottom the slope is monotonically increasing. This means that with increasing c additional terms start to contribute. It can be shown from eq. (13) that for small enough c the apparent ΔH should be linear in c. Plotting ΔH in this way, one finds indeed a straight line with an intercept at $c = 0$ of −5.3 kcal/mole. Eq. (13) provides a much more accurate way of determining ΔH^0. First one determines $A_1(T)$ for a number of temperatures, by plotting $\Delta\epsilon/c$ against c. At low concentrations one should find a straight line with slope $A_2(T)$ and intercept $A_1(T)$. In fig. 2 the low concentration data are presented in this way, for 12 temperatures ranging from top to bottom from −2°C to +48°C. The straight lines are least squares fits. One notices that A_2 is negative, as expected. The logarithms of the $A_1(T)$ values so determined are plotted against $1/T$ in fig. 3. It may be seen that the data are in excellent agreement with eq. (13), leading to a value for ΔH^0 of −5.1 kcal/mole. This value is also in good agreement with the less reliable value obtained by means of the extrapolation procedure mentioned above. At the same time fig. 3 allows us to determine ln $2\Delta\epsilon_e + \Delta S^0/R$ from the intercept. In principle this procedure

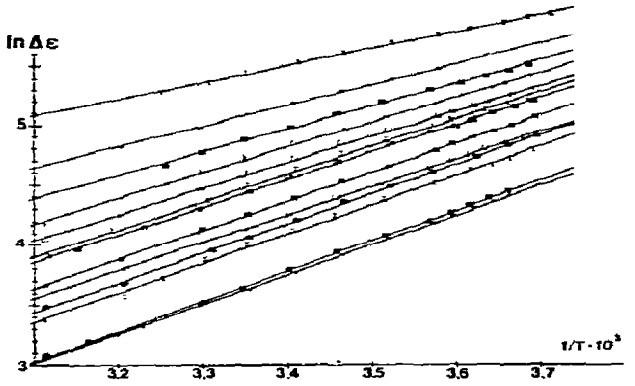

Fig. 1. Plot of ln $\Delta\epsilon_{288}$ versus $1/T$ for various concentrations of ATP. From bottom to top the weighed-in concentrations are, in units of 10^{-2} M: 1.004, 1.148, 1.425, 1.710, 1.890, 2.195, 2.68, 2.96, 3.22, 4.00, 5.03, 5.94, 10.00.

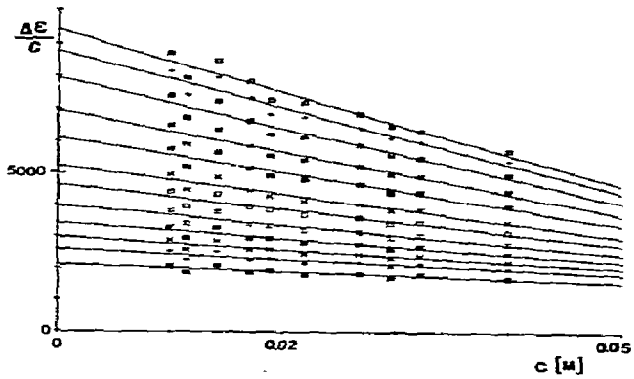

Fig. 2. Plot of $\Delta\epsilon/c$ versus c at various temperatures. From top to bottom the temperatures are: −2°C, 0°C, 3°C, 7°C, 11°C, 16°C, 20°C, 25°C, 30°C, 35°C, 40°C, 48°C.

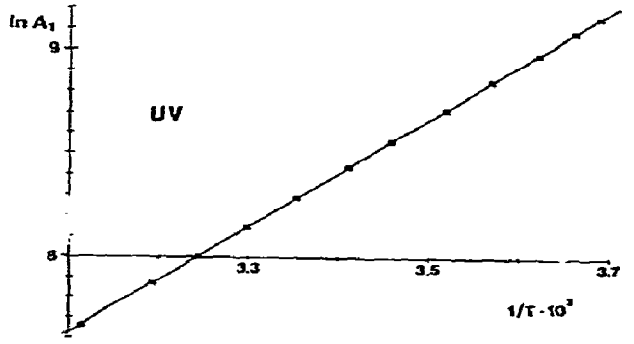

Fig. 3. Van 't Hoff plot for the UV expansion coefficient A_1.

could be continued: plotting $[\Delta\epsilon - A_1(T)c]/c^2$ against c, one could determine $A_2(T)$ and $A_3(T)$ from the intercept and slope of the straight line that should result. In this way one constructs very small quantities like $\Delta\epsilon - A_1(T)c$ which contain the total experimental error plus errors made in the determination of all previous A_i's.

In order to obtain $K_{25°C}$ and the spectroscopic parameters in a more reliable way, we performed a least squares fit with all the data, using the values of ΔH^0 and $\ln 2\,\Delta\epsilon_e + \Delta S^0/R$ as determined above from the low concentration data as fixed input values. Accordingly a least squares fit of the data was made to the complete expression (10) for the case of infinite non-cooperative association with $K_{25°C}$ and α as parameters, and to the expression (12) for the dimer case with $K_{25°C}$ as parameter. The best fit was achieved with $K_{25°C} = 8.4\,M^{-1}$ and $\alpha = 4.0$ for the case of infinite non-cooperative association. With K known, one can calculate $L = Kc$ for each concentration and temperature. Fig. 4 shows the $\Delta\epsilon$ values plotted versus L, together with the least squares fit to eq. (10). The fit using the dimer model was not as good (larger residual error), but this was not in itself considered to be sufficient evidence to reject this model. For the dimer model one gets $K_{25°C} = 2.1\,M^{-1}$. The data were not considered to be good enough to make a fit meaningful which allows an additional parameter to be adjusted (such as in the cooperative model).

The CD data were analyzed in essentially the same way. The construction of the difference spectra is

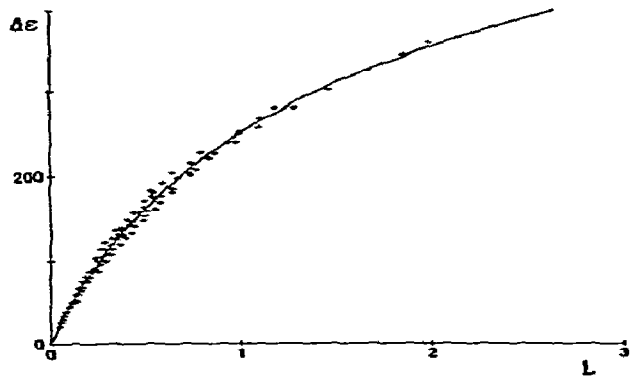

Fig. 4. UV extinction coefficient difference plotted versus $L = Kc$. The curve is the least squares fit for the model of indefinite non-cooperative self-association.

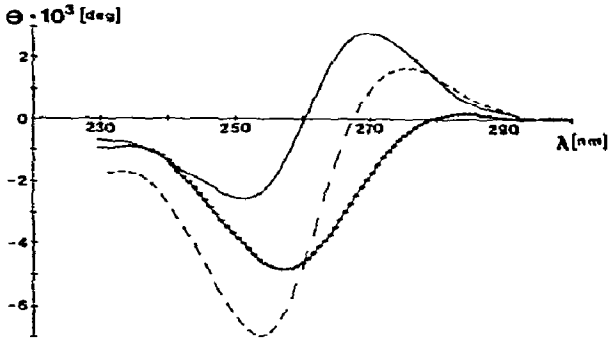

Fig. 5. CD spectra of ATP in 0.5 M $MgCl_2$, 1 M Tris/HCl at pH 8.7. (-----) CD spectrum of ATP at weighed-in concentration 1.148×10^{-2} M, measured in a cell of 0.1 mm path length; (+++++) CD spectrum of ATP at weighed-in concentration 1.148×10^{-4} M, measured in a cell of 1 cm path length; (——) CD difference spectrum.

straightforward and illustrated in fig. 5. By definition $\Delta\delta\epsilon$ is the difference between the CD signal of a partially associated sample and the CD signal of the same number of chromophores in the monomer state. Accordingly accurate measurements of the monomer CD spectra were needed. Fig. 5 shows that the monomer spectrum has an approximately gaussian band centered at the 259 nm ATP absorption maximum. Nine monomer spectra taken at various concentrations were normalized and averaged. These monomer spectra showed the expected Lambert–Beer behavior. A slight temperature effect was detected and corrected for. All manipulations on the spectra were performed using the Fourier program described in the previous section. At the ATP concentration of fig. 5, only monomers and dimers are present in measurable quantities. The shape of the difference spectrum remains approximately the same for all temperatures and concentrations used, i.e., a positive peak at 268.5 nm, a crossover at about 260 nm and a negative peak at about 252 nm. The temperature dependence at fixed concentration is shown in fig. 6. The maximum signal at 268.5 nm was used in our further evaluations. As above for the UV data, $\ln \Delta\delta\epsilon$ was plotted versus $1/T$. The resulting straight lines gave apparent ΔH values, which resulted in an extrapolated value of $\Delta H^0 = -5.2$ kcal/mole at zero concentration. Plotting $\Delta\delta\epsilon/c$ versus c gave the expected straight lines, which are shown in fig. 7 for various temperatures. The intercepts from these plots, $A_1(T)$, are logarithmically

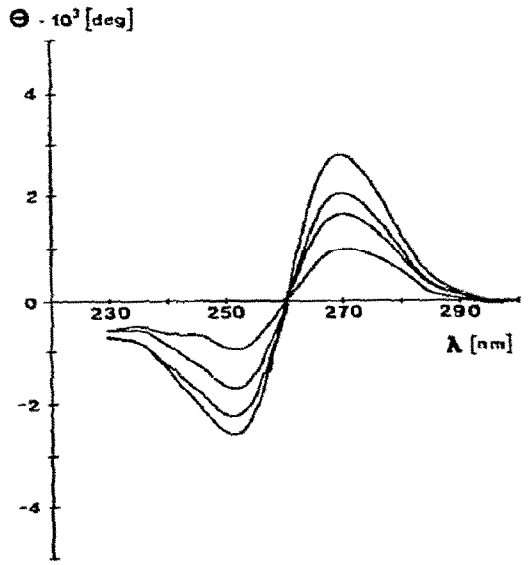

Fig. 6. CD difference spectra of 1.148×10^{-2} M ATP solution, measured in a cell of path length 0.1 mm, at various temperatures. At 268.5 nm the temperatures are from top to bottom: −4.5°C, +2.2°C, +9.8°C, +30.4°C.

plotted against $1/T$ in fig. 8. An accurate value of −5.1 kcal/mole for the dimerization enthalpy could be determined in this way. Using this value for ΔH^0 and the combination of ΔS^0 and $\Delta\delta\epsilon_c$ determined from the intercept in fig. 8, a least squares fit was made for all the data in order to determine the remaining parameters. A best fit for the case of indefinite non-cooperative association was achieved with

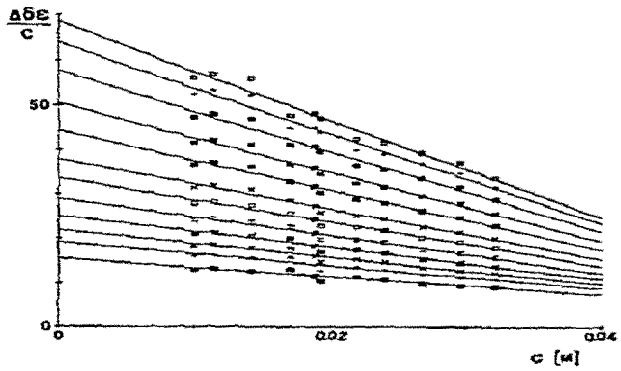

Fig. 7. Plot of $\Delta\delta\epsilon/c$ versus c at various temperatures. From top to bottom the temperatures are: −2°C, 0°C, 3°C, 7°C, 11°C, 16°C, 20°C, 25°C, 30°C, 35°C, 40°C, 48°C.

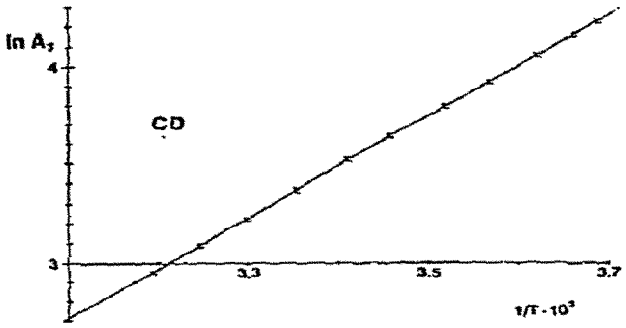

Fig. 8. Van 't Hoff plot for CD expansion coefficient A_1.

$\alpha = 2$ and $K_{25°C} = 8.0\,M^{-1}$. The dimer model allows a possible fit as well with $K_{25°C} = 4.0\,M^{-1}$.

The thermodynamic parameters determined in this way, together with the values for slightly different conditions of pH and ionic strength are summarized in table 2. A reduction of the ionic strength leads to a slight decrease in the association constant. No clear dependence on the type of salt is observed. The measurements at pH 7.7 show that no significant pH effect is present in this range. This is of some importance, since the pH of Tris buffer has a large temperature coefficient.

For the purpose of comparison, thermodynamic data for the self-association of a number of nucleosides and nucleobases in water are collected in table 3. The sign and order of magnitude of ΔH^0 and ΔS^0 for ATP is the same as for these compounds. The equilibrium constant is thus also of similar magnitude. It ap-

Table 2
Thermodynamic parameters for the self-association of ATP in various buffers

Buffer	pH	ΔH^0 (kcal/mole)	ΔS^0 (e.u.)	$K_{25°C}$ (M^{-1})
0.5 M $MgCl_2$ 1 M Tris/HCl	8.7	−5.1	−13.0	8.2
1 M NaCl 1 M Tris/HCl	8.7	−5.7	−15.7	5.6
1 M Tris/HCl	8.7	−5.6	−16.6	3.1
0.5 M $MgCl_2$ 1 M Tris/HCl	7.7	−5.5	−14.5	7.2

Table 3
Thermodynamic parameters of self-association in water

Compound	ΔH^0 (kcal/mole)	ΔS^0 (e.u.)	$K_{25°C}$ (M^{-1})
Purine [a]	−4.2	−13	2.1
Ribosylpurine [b]	−2.5	− 7	1.9
6-Methylpurine [a]	−6.0	−16	6.7
Deoxyadenosine [c]	−6.5	−18	4.7–7.5
N^6,N^9-Dimethyl-adenine [d]	−8.7	−21.6	45.6
ATP	−5.1	−13	8.2

a) Data from refs. [23] and [24].
b) Data from refs. [25] and [22].
c) Data from ref. [1].
d) Data from ref. [13].

pears that under the conditions of high ionic strengtl employed, the self-association is barely affected by charge effects.

Several reasons may be advanced for favoring the model with infinite self-association over the dimer model. There is no obvious physical reason why self-association should terminate at the dimer stage. Ultracentrifuge studies of AMP [3] and other adenine derivatives [16] show that aggregation occurs beyond dimer formation. The quality of the least squares fit is best for the infinite model. Fitting the UV and CD data with the dimer model leads to identical ΔH^0 values but different equilibrium constants for the two methods, whereas the infinite model leads to identical enthalpies and identical equilibrium constants.

Fig. 5 shows that the observed CD spectrum is indeed of the couplet type, and quite similar in shape to that of ApA. The amplitude is considerably smaller than for ApA. The least squares fit leads to a $\delta\epsilon$ value of 1.8 M^{-1} cm^{-1} per monomeric unit in the self-associated dimer, which is 5 to 6 times smaller than the corresponding value for ApA.

To interpret this value in terms of geometry, a set of dimer spectra was simulated using expressions (15), (16), (17) and (18). For Δ and $|\mu_1|$ we employed the values determined from the monomer absorption spectrum: Δ = 16 nm, $|\mu_1|$ = 3.92 D. Since the self-association is believed to occur via vertical stacking of the base moieties [1], even for the charged nucleotide AMP [2,17], we have adopted the model of a vertical stack with R_{12} perpendicular to the bases and equal to the van der Waals distance of closest approach (3.4 Å). This is also the value normally used in calculations on dinucleotides. With ω the angle between μ_1 and μ_2 (see fig. 9a), eq. (16) now simplifies to

$$R_{\pm} = \mp(\pi/2\lambda_0)|R_{12}||\mu_1|^2 \sin\omega.$$

Eq. (15) for V_{12} now reads

$$V_{12} = \frac{1}{|R_{12}|^3}|\mu_1|^2 \cos\omega.$$

CD spectra were simulated using these expressions, for various values of ω. Since $\delta = |\lambda_+ - \lambda_-|$ is smaller than Δ, the positions of the peaks are determined by δ rather than by Δ (as mentioned above) and are thus independent of V_{12} and of any approximation made in the calculation of V_{12}. A best fit to the dimer CD spectra was obtained with $\omega = 1.8°$ or $\omega = 181.8°$. Even if an appreciable error were made in the calcula-

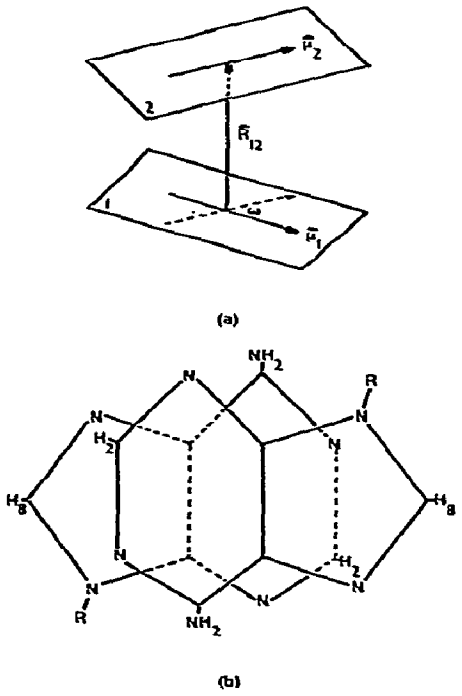

Fig. 9. (a) Geometry for vertical stack of two imaginary planar molecules. (b) Proposed head-to-tail stacking geometry for ATP. R stands for the sugar–phosphate rest.

tion of V_{12}, for instance due to our use of the dipole-dipole approximation, this would not materially affect our conclusion that the angle between the transition dipole moment directions is quite small. An even smaller angle would result if we had made the error of underestimating $|V_{12}|$, whereas an overestimation of $|V_{12}|$ by a factor of 10 would still lead only to an angle of about 18°. An error of this magnitude in V_{12} is quite unlikely, however, since the value of δ we calculated using the dipole-dipole calculation at $\omega = 36°$ as a control, is of a magnitude comparable to the one calculated for ApA in the same geometry by the monopole calculation [15,18]. In addition it is unlikely that the dipole–dipole approximation breaks down so dramatically at $|R_{12}| = 3.4$ Å.

We cannot arrive at a unique geometry on the basis of the CD data alone, however. Of the four possible geometries (head-to-head and head-to-tail each with $\omega = 1.8°$ or 181.8°), we feel that head-to-tail with $\omega = 181.8°$ is most likely. In this geometry, the phosphate charge repulsion, the repulsion between the permanent dipole moments, and steric hindrance are minimized. No NMR experiments have been performed as yet on the self-association of ATP, whereas on the closely related substance adenosine-5′-monophosphate (AMP) two such NMR studies exist [2,17]. Ts'o et al. [2] prefer a head-to-head geometry, with a small angle between the transition dipole directions, but cannot exclude the head-to-tail alternative. Their interpretation is consistent with our measurements and corresponds to one of our geometrical possibilities. The charge repulsion would seem to be larger in their model than in the one we prefer. Son and Chachaty [17] claim that the H_2 proton must be above the five membered ring and cannot be above the pyrimidine part, thus favoring the head-to-tail geometry with $\omega \approx 180°$ shown in fig. 9b. We emphasize that these NMR results refer to AMP rather than to ATP. In conclusion one may say that our CD measurements on ATP are consistent with the NMR measurements on AMP. No unique geometry could be assigned, but the number of possibilities could be reduced to four.

Acknowledgement

We wish to thank Professor G. Schwarz for helpful discussions and Mr. E. Volz for technical assistance.

This work was supported by the Swiss National Foundation (Schweizerischer Nationalfonds Kredit Nr.3.522.71).

Note added in proof

Recently a paper appeared on the self-association of 6-methylpurine [19]. In this study the equilibrium constant was determined by means of UV absorption measurements. Good agreement was obtained with the results of previous independent calorimetric [20, 21] and osmometric [7] measurements, thus showing that the results of the optical methods and the thermodynamic methods agree in this case. Meanwhile, we have also carried out absorption and CD measurements on the self-association of N-6-dimethyladenosine. The results of this study, to be published elsewhere, confirm the conclusions reached in this paper. Conservative CD spectra are again observed for the dimer. The thermodynamic parameters determined by the absorption and CD measurements agree amongst each other and with those derived from ultracentrifuge measurements [16] and osmometry [22]. It thus appears that the optical methods provide a reliable way to study the self-association of purine derivatives.

References

[1] P.O.P. Ts'o, in: Fine structure of proteins and nucleic acids, eds. G.D. Fasman and S.N. Timasheff (Marcel Dekker, New York, 1970) p. 49.
[2] M.P. Schweizer, A.D. Broom, P.O.P. Ts'o and D.P. Hollis, J. Amer. Chem. Soc. 90 (1968) 1042.
[3] G.P. Rossetti and K.E. Van Holde, Biochem. Biophys. Res. Commun. 26 (1967) 717.
[4] M.E. Magar, Data analysis in biochemistry and biophysics (Academic Press, New York, 1972) ch. 12.
[5] J. Kreuzer, Z. Phys. Chem. (Leipzig) B53 (1943) 213.
[6] J.A. Schellman, Compt. Rend. Trav. Lab. Carlsberg 29 (1956) 223.
[7] P.O.P. Ts'o and S.I. Chan, J. Amer. Chem. Soc. 86 (1964) 4176.
[8] R.F. Steiner, Arch. Biochem. Biophys. 39 (1952) 333.
[9] E.T. Adams Jr. and J.W. Williams, J. Amer. Chem. Soc. 86 (1964) 3454.
[10] J.A. Schellman, Accounts Chem. Res. 1 (1968) 144.
[11] I. Tinoco Jr., Rad. Res. 20 (1963) 133.

[12] B.H. Robinson, A. Löffler and G. Schwarz, Faraday Trans. I 69 (1973) 56.
[13] D. Pörschke and F. Eggers, Eur. J. Biochem. 26 (1972) 490.
[14] S. Tazawa, I. Tazawa, J.L. Alderfer and P.O.P. Ts'o, Biochemistry 11 (1972) 3544.
[15] W.C. Johnson Jr. and I. Tinoco Jr., Biopolymers 8 (1969) 715.
[16] R. Bretz, A. Lustig and G. Schwarz, Biophys. Chem. 1 (1974) 237.
[17] T. Son and C. Chachaty, Biochim. Biophys. Acta 335 (1973) 1.
[18] A.S. Schneider and R.A. Harris, J. Chem. Phys. 50 (1969) 5204.
[19] G.R. Kelly and T. Kurucsev, Biopolymers 13 (1974) 769.
[20] P.R. Stoesser and S.J. Gill, J. Phys. Chem. 71 (1967) 564.
[21] M.G. Marenchic and J.M. Sturtevant, J. Phys. Chem. 77 (1973) 544.
[22] A.D. Broom, M.P. Schweizer and P.O.P. Ts'o, J. Amer. Chem. Soc. 89 (1967) 3612.
[23] S.J. Gill, M. Downing and G.F. Sheats, Biochemistry 6 (1967) 272.
[24] P.O.P. Ts'o, I.S. Melvin and A.C. Olson, J. Amer. Chem. Soc. 85 (1963) 1289.
[25] E.L. Farquhar, M. Downing and S.J. Gill, Biochemistry 7 (1968) 1224.